MODELING AND SIMULATION OF FLAPPING WINGS MICRO-AERIAL-VEHICLES FLIGHT DYNAMICS

Jerzy Lewitowicz, Grzegorz Kowalczyk, Krzysztof Sibilski, Jozef Zurek
Air Force Institute of Technology

Keywords: *flight dynamics and control, micro aerial vehicles, biomimetics*

Abstract

The objective of this paper is to present possibilities of transferring to flapping wings micro aerial vehicle (FMAV) flight dynamics methods applied to flexible structure control in aeronautics. Two important aspects of the problem are considered: structure modelling and modern control methods. The old Wright Brothers' idea of wing twisting to achieve a specified roll rate is examined in a new arena of FMAV manoeuvres. Therefore, we present key aspects of the active flexible wing technique. Equations of motion for flexible FMAV wings, coupled to a rigid supported "fuselage" are developed, and some results of simulations are presented.

1 Introduction

The development of small autonomous flying vehicles is motivated by a need for intelligent reconnaissance robots, capable of discreetly penetrating confined spaces and maneuvering in them without the assistance of a human telepilot. Without pilot and only equipment on board, unmanned aerial vehicles may be much smaller then "normal" aircraft. This induces interest to the concept of *micro air vehicles* (MAV or μAV or micro-flyer) with wingspan of 15 cm or less. Such aircraft are considered to be efficient and inexpensive tools for collecting information in dangerous or hostile environments. For instance, equipped with a sensory device, such an aircraft could be used to detect the presence of poisonous gases in an environmental disaster area or if equipped with a camera, it could be used in a short endurance reconnaissance mission of interest to the military. In either case, the focus is on reducing the size of such aircraft as much as possible.

The MAV is of comparable size of birds and insects. It stimulates interest of designing the flapping wing for MAV as an attractive alternative for fixed or rotating wing configurations. The current research on animal-like MAV resulted in the new term animalopter, describing similarity of MAV to real animal. An animalopter means the animal-like flying objects with moving wings. An animal (i.e. bird, bat or/and insect) wing is a multifunctional device providing lift, propulsion and flight control and performing complex motion relative to the "aircraft" body, which shows the analogy to helicopter rotor [9].

In the background of preparing this paper lies our believe that transferring ideas from the more matured disciple like aircraft technology to emerging animal technology should be beneficial for the later one and vice-versa. One integrated idea, of special interest to both disciplines, is the *active flexible wing* concept. This concept represents a return to the Wright Brothers' idea of wing warping or twisting by combining wing structures and flight controls to perform the desired manoeuvres.

Whether cruising trough an open field or circling garbage, flies impress us with their remarkable aerodynamic manoeuvrability. How is this sophisticated flight control achieved? Like all well-controlled locomotory systems, flies must rapidly integrate incoming sensory information and appropriately modify their motor output.

It is well known that the dynamics of flapping wings MAV over the flight envelope is highly nonlinear. The character of the loads acting on the vehicle - particularly the

aerodynamics - vary substantially over the angle of attack operating range (which may nowadays include poststall incidences). The control of this type of plant can be achieved adequately via a variety of approaches, provided that the parameters of the controller (the gains in particular) are scheduled with flight condition. The nonlinearity of the system makes it difficult to implement a strategy of interpolating between gains derived from a few choice trim points. This is because the plant and the controller interact such that it is not clear precisely what the closed loop trim points are in vide flight regions, because aerodynamic loads often become asymmetric and where inertial coupling is significant.
The primarily goal of our work is to developed the software simulation for flapping wings micro aerial vehicle. This simulator is an end-to-end tool composed from several modular blocks, which model: wings aerodynamics, the body motion, and control algorithms.

2 The Main Issues

2.1 Animal flight vs aircraft flight

There is some subtle but important difference between animal and aircraft models. In biological flight the wings not only move forward relative to the air, they also flap up and down, plunge, and sweep. Conventional airplanes with fixed wings are in comparison very simple. The forward motion relative to the air causes the wings to produce the lift. Animals do not, in general, have rotating parts that describe a full circular motion. To attain the appropriate effective angle of attack throughout the entire wing-stroke, the wings must constantly twist.

2.2 Mission Performance Constraints

Results of some optimisation studies show that the vehicle size is highly sensitive to the minimum required turning radius because vehicles that must turn tightly require lower wing loading, which implies greater size for a fixed total mass.
The missions requires the vehicle to fly a distance of approximately 1000 m from the launch site to capture a clear image of a 1.5-m-size target on the ground, and to deliver that image to the launch site in less than 45 min. However, the mission profile includes not only cruse to target, and return to launch site, but also dive and climb over the target. The MAV in the vicinity of the target must make several shallow dives and climb to view and transmit a clear image of the target before return and landing. Therefore the MAV must be able to efficiently and safely navigate in 3-dimentional space among obstacles (e.g. trees) to a target location.

2.3 Features of Airfoil for Animals

The typical airfoils for birds and bats are thin and cambered, which means that these generate very little leading-edge suction. Cruising birds and bats fly with their flapping axes aligned close to horizontal. This could produce an interesting dilemma for the upstroke.
Insects have low-aspect-ratio wings, which are not suitable for cruising flight. During the downstroke, the insect generates mainly a vertical force. The acceleration of the insect's body during the first half of the downstroke is especially large, and this acceleration is mainly caused by a large unsteady pressure drag action on the wings. During the upstroke the insect generates mainly a horizontal force. The change of direction of the forces during the down-and-up-strokes is controlled by variation in the inclination of the stroke plane.

2.4 Aerodynamic Phenomena

As the size of an aircraft is reduced the need of efficiency in terms of lift and propulsion generation becomes more evident. Reducing the size of lifting surfaces and keeping the flight speed around 15 m/s makes the aerodynamic phenomena different from those found in normal size aircraft, mainly due to very low Reynolds number of the flow.
Moreover, animalopter maneuvering in this regime are subject to nonlinear, unsteady aerodynamic loads [2, 12]. The nonlinearities and unsteadiness are due manely to the large

regions of 3-D separated flow and concentrated vortex flows that occur at large angles of attack. Accurate prediction of these nonlinear, unsteady airloads is of great importance in the analysis of an animalopter flight motion and in the design of its flight control system.

Prediction of the unsteady airloads is complicated by the fact that the instantaneous flowfield surrounding a maneuvering body, and thus the loading, is not determined solely by the instantaneous values of the motion variables, such as the angles of attack and sideslip, and, particularly in our study, by the deforming flexible wings parameters. In general, the instantaneous state of the flowfield depends on the time-history of motion, that is, on all the states taken by the flowfield during the maneuver prior to the instant in question.

2.5 Beam or Plate Model of Flapping Wings

During designing of animalopters, various configurations must be evaluated to determine the characteristics of the configuration that will meet all requirements of vehicle performance and cost.

A problem generated by model of a plate arises. For plates made from composites, the number of layers and the fibber orientation may be assumed arbitrary, which vary the amount of coupling between and twisting. In classical plate theory these significant effects are not accounted for either in deflection equations or in boundary conditions.

2.6 Control Problems

The co-evolution of form and function is the way all living organisms evolved in nature. in nature's example is to be followed, the form and function of autonomous agents be co-evolved in similar manner [1].

Design of an animalopter wing requires solving various problems:

1. Controllability of the flight in adverse conditions: icing, rain, wind.
2. How to build simpler control systems using "active materials"?
3. Whether the well-known methods for aircraft flight control and stabilisation may be adapted to animalopter?

During flight the aircraft is expected to encounter turbulent winds up to 10 m/s, perform tight turns near buildings, and climb repeatedly to 100 m. The aircraft must be stable enough to serve as a live airborne video platform and must be easy enough to fly so that an individual with minimal training can operate it.

2.7 How to Describe Animalopter Manoeuvres?

As can be seen in Sec. "Co-ordinate systems", attitude angles, which represent the instantaneous flight attitude of an animalopter are included. The most common angles are, of course, Euler ones. The tree Euler angles Φ, Θ and Φ, used in flight mechanics are called "roll angle (bank angle)", "pitch angle", and "yaw angle (heading angle)", respectively.

On the other hand, the terms *rolling*, *pitching*, and *yawing* mean the angular motions about the animalopter-fixed axes. These motions are usually described by the angular velocity components P, Q, and R, respectively. Then, by how many degrees of angle does a manoeuvring animalopter rotate about each axis from one moment to another? These rotation angles are not equal to the variations of Euler angles during that time! In the fact, the Euler angles are kinds of rotation angles. However, those define a special rotation sequence and not, in general, the rotation angles of the actual rotation sequence at that time.

For another problem, when we consider two flight attitudes that are described by Euler angles Φ, Θ and Ψ, how do we compare the two attitudes? Are those attitudes near or far? How is the relative attitude viewed from one attitude to another? These questions may occur to anyone who tries to treat large maneuvers more precisely. But the problem with angles is not as easy to handle as problems with other physical quantities [3, 5].

2.8 Degrees of freedom

Not only at first sight, the study of animalopter flight dynamics and control may seem very complicated, since each wing possesses degrees of freedom in addition to those of the

"fuselage". Detailed analyses of kinematics are central to an integrated understanding of animal flight. Four degrees of freedom in each wing are used to achieve flight in the Nature: flapping, lagging, feathering, and spanning.
Flapping is a rotation of animal wing about longitudinal axis of the animal body (this axis lies in the direction of flight velocity), i.e. this is "up and down" motion. Lagging is a rotation about a "vertical" axis; this is the "forward and backward" wing motion backward parallel to the body. Feathering is an angular movement about the wing longitudinal axis (which may pass through the wing centre of gravity) which tilts the wing to change its angle of attack. Spanning is an expanding and contracting of the wingspan. Not all flying animals perform all of these motions. For instance insects with low wing flap frequencies about 20 Hz (17…25 Hz) generally have very restricted lagging capabilities. Unlike birds, most insects do not use the spanning technique.
Insects such as alderfly (Apatele alni) and mayfly (Ephemera) have fixed stroke planes with respect to their bodies. Thus, flapping flight is possible with only two degrees of freedom: flapping and feathering. In the simplest physical models heaving and pitching represent these degrees of freedom.
The motion of each bird wing may be decomposed into flapping, lagging, feathering (the rigid body motions) and also into more complex deflections of the surface from the base shape (vibration modes).

3 Description of Control Problem

3.1 Aeroelastic Nature of Control Problem

Very recently, it has been recognised that flapping wing propulsion can be more efficient than conventional propellers if applied to MAVs, because of the very low Reynolds numbers encountered on such vehicles. Flapping flight is more complicated than flight with fixed or rotating wings. The key to understand the mechanisms of flapping flight is the adequate physical and mathematical modeling.

The wing shape can be controlled by the deflection of the piezo-ceramic bender the applied DC voltage. Simultaneously, the flexible wing exposed to the airflow will also deform under the resultant aerodynamic force acting on its upper and lower surfaces. The wings can therefore be modelled as a uniform cantilever composite beam subjected to two types of loads: aerodynamic pressure, and bending moment generated by piezo-electric action. The problem is thus "aero-elastic" in nature (Fig. 1).
From the point of view of mechanical phenomena involved, loads causing motion of the structure are: aerodynamic (A), inertial (I) (gravity included), and elastic (E) (Fig. 2 left). These loads act on both aeronautical and animalopter structures, so mathematical models considered in both fields may be similar. The interaction between an aircraft's structural dynamics, aerodynamics, and automatic flight control system has emerged as an important design consideration. This interaction is called aeroservoelasticity and is illustrated by Fig. 1 right (from Ref. [7]).

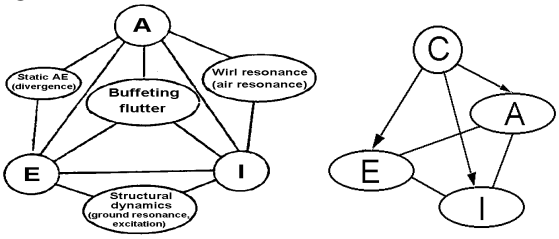

Fig. 1 Aeroelastic phenomena (left) and aeroservoelastic tetrahedron (right)

Both branches of knowledge (aeronautics and zoology) have been developing separately, with almost no information transfer between them. As there are some points of common interest (structure modelling, loads, methods of control) it seems useful to look at modelling of animalopter dynamics from the point of view of aeronautics to define places, where "technology transfer" is possible.
This is for instance an aeroelastic tailoring, which, with structure optimisation, develops recently very intensively. The active methods, which emerged recently, are based on application of integrated active/sensor "smart" elements [8].

This calls for the use of MDO (*multidisciplinary design optimisation*) methodology, which takes advantage of the synergism among various disciplines in a complex system in order to arrive at an optimal design. In applying MDO to aircraft design, aerodynamics structures, flight mechanics, and propulsion are some of the disciplines commonly considered.

3.2 Biological Inspiration of MAV Design

Before dealing with the flight dynamics and the control problem analytically, let us consider the physical effects of wing motions on the animalopter.

To investigate how birds with different morphology change their wing and body movements while flying at a range of speeds. , Tobalske and Dial [13] analysed high-speed video tapes of black-billed magpies (Pica pica) flying at speeds of 4 – 14 m/s and pigeons (Columba livia) flying at 6 – 20 m/s in a wind tunnel.

Many flying machines from self-inflating parawings to birds are using lifting surfaces that significantly deform. With the right choice of materials, prestress, and unstrained shape, an aerodynamically effective equilibrium configuration can often be achieved to improve the flight performance.

Wings of insects may have various shapes, but their internal structure is similar for the majority of species. Usually the insect wing is composed of two membranes. It is a sandwich structure with two layers made from chitin of the thickness of micrometer order. The fibres going along the span fold the surface. These fibres, concentrated mainly in the vicinity of leading edge, act as stiffening elements and may form various patterns. For instance the fibres in dragonfly wing go mainly along the span and are inter-connected with small cross-fibres (similar to ribs in aircraft structure). These ribs are more densely grouped close to wing leading edge (Fig.3).

The stiffness and the shape of an insect wing are variable and may be controlled. At the rest the wing is flat, but it changes the shape during flight.

The insect body has the muscles providing the forces to power the wings and performing variation of wing shape. The skin of the body forms a closed box, within which the "bearings" for wing roots are placed.

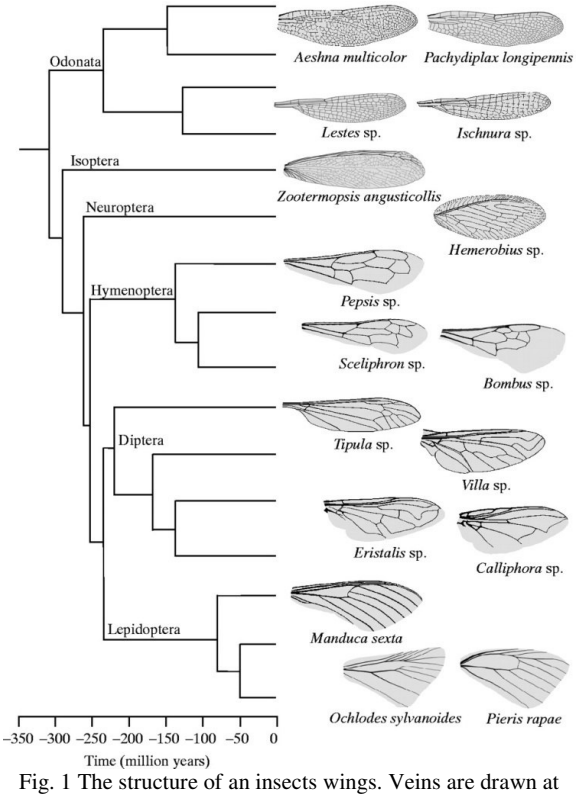

Fig. 1 The structure of an insects wings. Veins are drawn at actual thickness; wings are not shown to scale. Genus and species names (when known) are shown under each wing, and orders are listed at their branching points (cf. Combes & Daniel [13])

The fields of Biology that use principles of Structural Engineering and Fluid Mechanics to draw structure - function relationships are Functional Morphology or Biomechanics. These disciplines are of particular use to Bionics engineers, because the behavior and performance of natural structures can be characterized with methods and units that are directly applicable to mechanical analogs. The result of precise spatial and temporal regulation is a complex exoskeleton that is tagmatized into functional zones. Limbs consist of tough, rigid tubes made of molecular plywood, connected by complex joints made of hard junctures separated by rubbery membrane. The most elaborate example of an arthropod joint is the wing hinge,

the morphological centerpiece of flight behavior (see fig. 3).

Fig. 3 shows hinges system of flying insects. The horizontal hinge ① occurs near the base of the wing next to the first axillary sclerite. This hinge allow the wing to flap up and down. The vertical hinge ② is located at the base of the radial vein near the second axillary sclerite (2AX), and is responsible for the lagging motions of wing. The torsional hinge ③ appear to be more complicated interaction of sclerite and deformable folds.

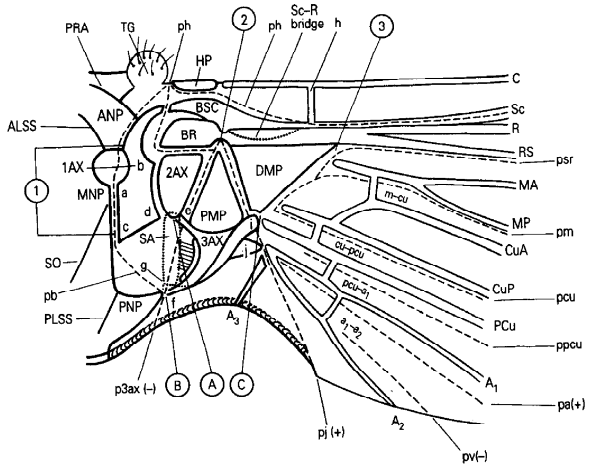

Fig. 4 Insect Axillary Apparatus. Region at the base of the wing containing all the intricate mechanical components. First axillary sclerite (1AX), articulates with the anterior notal process and forms the horizontal hinge. Second axillary sclerite (2AX) articulates with an extension of the thoracic wall. The 2AX is responsible for the pleural wing process (PWP), and support the radial vein, (main mechanical axis for the wing). Third axillary sclerite (3AX) is responsible fopr wing flexing, and play role of the vertical hinge.

The hinge consists of a complex interconnected tangle of five hard scleratized elements, imbedded within thinner, more elastic cuticle, and bordered by the thick side walls of the thorax. In most insects, the muscles that actually power the wings are not attached to the hinge. Instead, flight muscles cause small strains within the walls of the thorax, which the hinge then amplifies into large oscillations of the wing. Small control muscles attached directly to the hinge enable the insect to alter wing motion during steering maneuvers. The indirect muscles do not directly effect wing. They are attach to the tergum, and distort the thoracic box when contracted. This distortion transmits forces to the wing. There are two bundles of indirect muscles: dorsolongitudinal (DLM), and dorsoventral (DVM). The dorsolongitudinal muscles span the length of the tergum, the dorsoventral muscles extend from the tergum to the sternum. The direct muscles connect directly from the pleuron (thoracic wall) to individual sclerites located at the base of the wing. The subalar and basalar muscles have ligament attachments to the subalar and basalar sclerites. Resilin is a highly elastic material and forms the ligaments connecting flight muscles to wing apparatus, and it is 100 times greater energy storage capabilities than muscle. There are other muscles that are directly inserted into the first and third axillary sclerite (see fig. 5)

Although the material properties of the elements within the hinge are indeed remarkable, it is the structural complexity as much as the material properties that endow the wing hinge with its astonishing characteristics. Sometimes it is not the actual morphology that endows a biological structure with its functional properties, but the intelligence with which it is used. Intelligence does not necessarily imply cognition; it may simply reflect the ability to use a structure in an efficient and flexible manner.

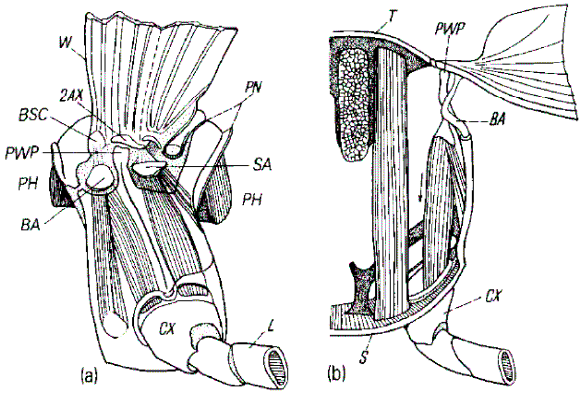

Fig. 5 The direct flight mucles within the wing bearing segment: (a) lateral view; (b) crosssectional view.

Although most biological structures are not intelligent by human standards, they nevertheless outperform most bricks and I - beams. A good example is the insect wing (fig. 6). The wing is the structure with membranous cuticle stretched between veins in the wing. Unlike an aircraft wing, it is neither streamlined nor smooth. Folds facilitate deformation during flight. Veins increase the mechanical rigidity of the wing (alternate in concave and convex

patterns). Radial vein is the longitudinal rotational axis of the wing, about which occur pronation and supination.

Engineers and biologists have long struggled to explain how a bumblebee (or any insect) remains in the air by flapping its wings. Conventional steady-state aerodynamic theory is based on rigid wings moving at a uniform speed. Such theory cannot account for the force required to keep an insect in the air. The solution to this paradox resides not in the intrinsic properties of wings, but rather in the way that insects use them. By flapping the wings back and forth, insects take advantage of the unsteady mechanisms that produce forces above and beyond those possible under steady-state conditions. Several research groups are actively attempting to construct miniature flying devices patterned after insects. Their challenge is not simply to replicate an insect wing, but to create a mechanism that flaps it just as effectively. Intelligent structures do not always function the same way; they adapt to local functional requirements. Even the simplest plants and animals sense their world, integrate information, and act accordingly. Feedback-control mechanisms are extremely important features that endow organisms with flexibility and robustness. Even plants, which lack a nervous system, can nevertheless grow leaves and branches toward light, roots toward water, or spatially regulate growth so as to minimize mechanical stress. The functions of biological structures cannot be fully understood or accurately mimicked without taking this complex dynamic feedback into account. Of all the properties of biological entities (with the possible exception of self-replication), it is their intelligence and flexibility that is perhaps the most difficult to duplicate in an artificial device. The next decade should be exciting for the field of Bionics. Just as biologists are discovering the structural and physiological mechanisms that underlie the functional properties of plants and animals, engineers are beginning to develop a fabrication tool kit that is sophisticated enough to capture their salient features. As the performance gap between biological structures and our mechanical analogs shortens, engineers may feel increasingly encouraged to seek and adopt design concepts from Nature. Although the devices they construct may at first appear alien, their origins in the organic world may endow them with an odd familiarity.

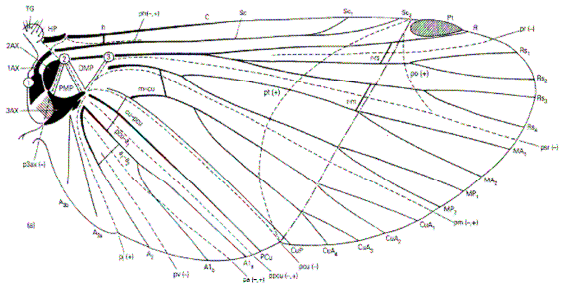

Fig. 6 The insect wing layout

Flying insects use flapping wings to attain amazing capabilities for hovering and maneuvering. Most of the recent work on Biological Micro Aerial Vehicles (BMAVs) bas been on the scale of avian flight which is quite different from insect flight. Notable examples in this list include the Caltech RTCLA Omithopter (Pornsin-Sirirak et al [30]), the Delf University of Technology (R. Ruijsink) [www.delffly.nl], the Georgia Tech Entomopter (Michelson) [23, 24], the Arizona University (Shkakaryev) [18], the France ROBUR project [6, 19] . The UC Berkeley developed the Micromechanical Flying Insect (MFI) project. This BMAV distinguishes itself with a wingspan of only 25 mm, almost an order of magnitude smaller than all the others (this translates into roughly three orders of magnitude difference in mass). The work on the MFI has been documented in a number of areas including design and fabrication, actuator development, thorax dynamics, sensing, and aerodynamic simulation [13, 32, 33, 34, 46, 47].

The success of insect-scale BMAVs depends on exploitation of unsteady aerodynamic mechanisms (in particular, delayed stall, rotational lift, and wake capture) which have only recently been elucidated by Dickinson et al [7, 8]. There has been some success with computational methods to estimate forces generated by flapping wings [9, 10, 29, 32, 36] but both the models and algorithms need to be improved in order to get better agreement with experimental values. The only reliable means to

determine the forces generated by the flapping wing is to measure them directly.

We can stated, that wings of an animalopter are a multifunctional devicesd, which create not only the aerodynamic lift, but also thrust, and, last but not least, can control the flight. Because of the complex equipment mounted on the animalopter, we can be stated, that the animalopter is a *flying micro-electro-mechanical robot*. We are dealing with an *entomopter,* if it is an artificial insect, or an *ornitopter,* if we are dealing with an artificial bird.

Animalopter is of dimensions similar to the dimensions of a small bird (or a bat) and a large insect. The thing that distinguishes animalopter from an ordinary radio-controlled small aeroplane are air operations, usually beyond the operator's sight range and on *small* Reynolds numbers (of the order of ten to a hundred thousand). The data of how the motion of wings and the body change during flight is interesting not only *per se,* but also in order to understand the mechanisms, which take place during flight and their mathematical modelling.

If one wanted to search for analogies with artificial objects, then because of the complex motion in relation to the body, animalopter is more similar to a helicopter that to an aeroplane. Therefore many concepts stemming from helicopter flight mechanics found use in flight biomechanics, of course after taking into account animalopters' specificity.

Bird's wing anatomy is quite well known and described. Feathers create a lifting surface with a highly complex structure and shape, which causes the entire wing to become a lifting surface of elastic and permeable profile, with numerous vortex diffusers, such as down and elastic feather radiuses. Moreover appropriate motions of the wings enable a change of their span, lift and sweep during flight, and motions of muscles and tendons inside the wings enable among others a change of camber of a wing profile. Analogously to insects, birds are also able to actively control the flight. Thanks to appropriate wing motions and arrangement of feathers they control the flow around the wings. The aim of this action, as in the case of insects, is minimalising of power needed for flight, reaching maximal velocity or maneouvrability, or fulfilling the requirements of flight in special conditions.

3.3 Flapping Wings Degrees of Freedom

Insect wing motion appear to be not simply up and down. It is much more complex (see fig. 7). Fig. 7 shows insect's wing tip trajectory. Such complex motion can be considered as being composed of three different rotations: flapping, lagging, feathering, and spanning. Flapping is a rotary motion of the wing around the longitudinal axis of the animalopter (this axis overlaps with the direction of flight velocity). Thus "up and down" motion is realised. Lagging is a rotary wing motion around the "vertical" axis, i.e. it describes "forward and backward" motion. Feathering is a rotary motion around longitudinal wing axis. During that motion changes of attack angle of the wing occur.

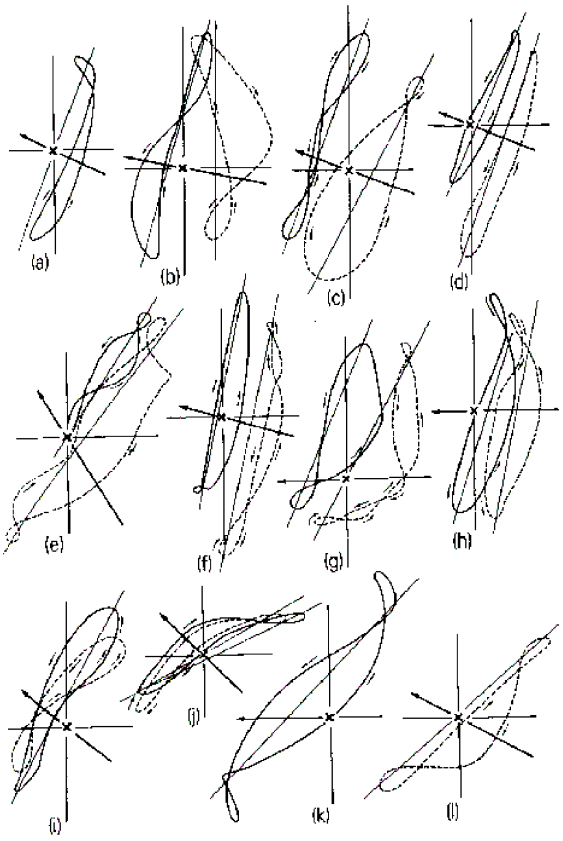

Fig. 7 Wingtip trajectories

Detailed analyses of kinematics are central to an integrated understanding of animal flight [1, 2,

8, 9, 10, 17, 20, 21, 25, 26, 27, 28, 32, 35, 37, 38, 39, 40]. Concluding, four degrees of freedom in each wing are used to achieve flight in the Nature: flapping, lagging, feathering, and spanning. This requires a universal joint similar the shoulder in a human. A good model of such joint is the articulated rotor hub (Fig. 8). Flapping is a rotation of a wing about longitudinal axis of the body (this axis lies in the direction of flight velocity), i.e. "up and down" motion. Lagging is a rotation about a "vertical" axis, this is the "forward and backward" wing motion. Feathering is an angular movement about the wing longitudinal axis (which may pass through the wing centre of gravity). During the feathering motion the wing changes its angle of attack.

Similar to insets, the motion of a bird wing may be decomposed into: flapping, lagging, feathering (the rigid body motions) and also into more complex deflections of the surface from the base shape (vibration modes) (see Fig. 7).

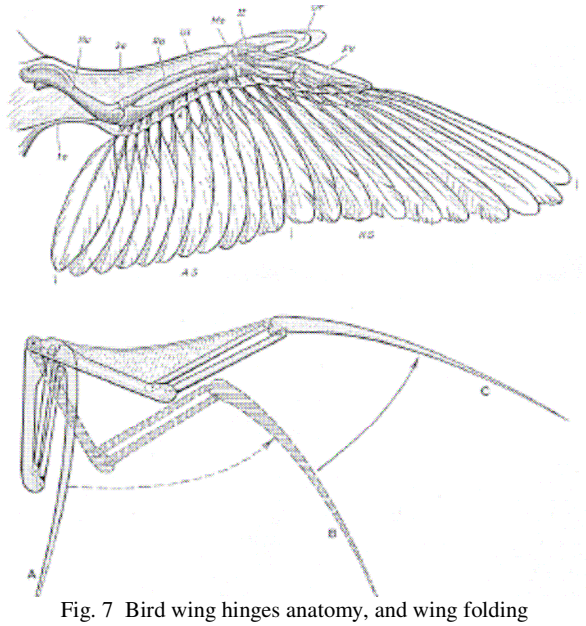

Fig. 7 Bird wing hinges anatomy, and wing folding

Insects with wing beat frequencies about 20 Hz generally have very restricted lagging capabilities. Insects such as alderfly (*Apatele alni*) and mayfly (*Ephemera*) have fixed stroke planes with respect to their bodies. Thus, flapping flight is possible with only two degrees of freedom: flapping and feathering. In the simplest physical models heaving and pitching represent these degrees of freedom. Spanning is an expanding and contracting of the wingspan. Not all flying animals implement all of these motions. Unlike birds, most insects do not use the spanning technique.

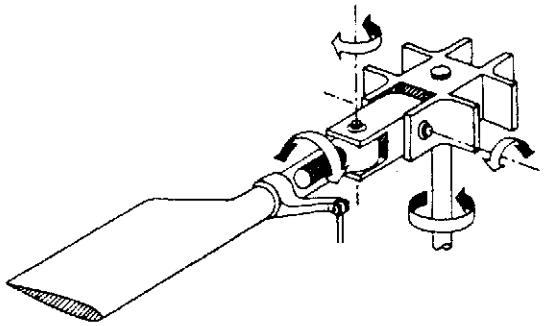

Fig. 8 Articulated joints of a helicopter main rotor hub

Spanning is a motion, which causes changes of wing aspect ratio. Not all animalopters use these motions. Unlike the birds, most insects do not use this technique. A significant question arises: which of these motions should be taken into account to obtain adequate description?

During level flight a bird has to flap its wings to generate aerodynamic lift and thrust to overcome terrestrial gravity force and drag. Instantaneous forces on the wings change during the cycle because of the changes of wing shape, deformability of joints, attack angle, turning of the wings, rotary velocity of the wings, elastic properties, flight velocity etc. A key issue here is the understanding of how complex motions of so complicated object generate aerodynamic forces. No wonder, that aerodynamics of flapping wings is thought to be the most difficult field of aeroplane and helicopter aerodynamics. The issue is further complicated by the fact, that this is an aerodynamics of small Reynolds numbers. It also needs to be emphasized, that conventional flight mechanics can only be a guide and not an authority while analysing animalopter's flight dynamics. It is enough to realise, that the moments of inertia of movable parts change, and, moreover, the changes are different on each wing. Geometric parameters also undergo changes, e.g. wing aspect ratio. Stabilization of motion is a serious problem. A way to understand animalopters' motion is a thorough kinematic, which is connected with the choice of levels of freedom. An extremely serious

problem is controlling such an object. This is caused by the fact, that wings do not have typical control surfaces, like ailerons (not to be confused with a kind of feathers!). Influencing the motion is possible only by changes of amplitudes and frequencies of flapping and turning the wings. It has been observed, though, that anima lots are capable of performing incredible acrobatic manoeuvres, which would not be possible without appropriate "control devices". Knowledge on this topic is in the process of being gathered.

Insects fly by oscillating (plunging) and rotating (pitching) their wings through large angles, while sweeping them forwards and backwards. The wingbeat cycle (typical frequency range: 5 - 200 Hz) can be divided into two phases: downstroke and upstroke (see Fig. 9*a*).

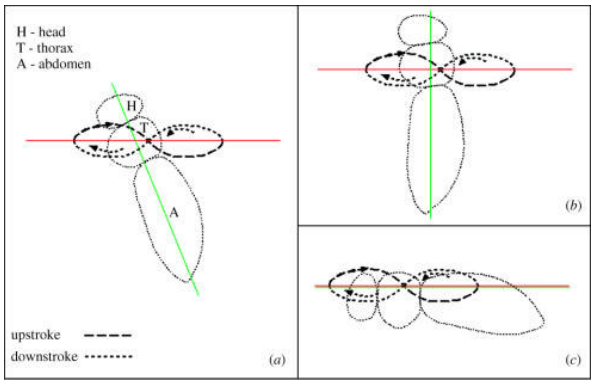

Fig. 9 Generic kinematics of insect in hover: the wing tip traces a 'figure-of eight', when seen from the insect side. The angle between the insect body axis (green) and the stroke plane (red) is constant. Typically, (*a*) the angle is steep; (*b*) one extreme: the angle is $\pi/2$; (*c*) the other extreme: the angle is zero (see Żbikowski and Galiński [48]).

At the beginning of downstroke, the wing (as seen from the front of the insect) is in the uppermost and rearmost position with the leading edge pointing forward. The wing is then pushed downwards (plunged) and forwards (swept) continuously and rotated (pitched) at the end of the downstroke, when the wing is twisted rapidly, so that the leading edge points backwards, and the upstroke begins. During the upstroke, the wing is pushed upwards and backwards and at the highest point the wing is twisted again, so that the leading edge points forward and the next downstroke begins.

Insect wing flapping occurs in a stroke plane that generally remains at the same orientation to the body. The actual angle corresponding to the orientation is an interesting design parameter, (see Fig. 9b, and 9c).

In hover the downstroke and upstroke are equal, resulting in the wing tip approximately tracing a figure-of-eight (as seen from the insect's side). However, the figure-of-eight is not necessarily generic, as other, less regular, closed curves with more than one or no self-intersections are also observed [48]. For two-winged flies (Diptera) a 'banana' shape seems to be common. However, even for Diptera the kinematics in hover can be more complicated, so we settled on the figure-of-eight as 'commonly occurring' for reference purposes.

Since each half-cycle starts from rest and comes to a stop, the velocity distribution of the flapping is non-uniform, making the resulting airflow complex. It is also unsteady, i.e. the aerodynamic force varies in amplitude and direction during each wingbeat cycle. The variability of the force is compounded by the strong influence of the viscosity of air (owing to the small scale) and significant interaction of the wing with its wake (owing to hover). Finally, it is worth mentioning that the thorax–wing system in true flies (Diptera) is resonant, which contributes to the efficiency of propulsion. This feature was not implemented in the presented mechanism, but it is considered for a future design in the form of electro-mechanical resonance.

Insect wing kinematics are essentially spherical, while the trace of the wing tip is usually photographed from the insect's side. The result is an orthogonal projection of the spherical trace on to the plane of the animal's longitudinal symmetry. The resulting planar figure for a hovering insect's wing is always closed. As far as can be discerned from the available (noisy) data, e.g. for flies, the actual shape may be a figure-of-eight or a banana shape, but can be irregular and sometimes the trace has no self-intersections. Owing to the inherent experimental difficulties, the kinematic and aerodynamic data from free-flying insects are sparse and uncertain, and it is not clear what aerodynamic consequences different wing motions have, despite notable progress (e.g. Dickinson et all. 1998; Lehmann & Dickinson

1998; Lehmann 2004). Since acquiring the necessary kinematic and dynamic data remains a challenge, a synthetic, controlled study of insect-like flapping is not only of engineering value, but also of biological relevance.
There are two phases in each half-cycle of the wing beat: translational (wing moving forwards or backwards) and rotational (at the end of each stroke). In order to clearly investigate the distinct aerodynamic contributions of each phase, the angle of attack should be constant during translation and rotate through at least 90° during the flip-over. Thus, theoretically attractive kinematics should entail an intermittent rotational motion with reversal. A more subtle aspect is the plunging (up–down) component of flapping. Every time a hovering wing starts (or stops) it sheds a starting (stopping) vortex (Wagner 1925; Żbikowski 2002b) which is then convected according to the airflow evolution. Despite the convection, such a vortex may persist in the vicinity of its original shedding point when the wing revisits that point in the next half-cycle. Then the wing and the vortex will collide and the flow structure is impaired. However, if the wing plunges up and down while moving forwards and backwards, it may be able to avoid hitting the vortex when revisiting the shedding point. In other words, figure-of-eight kinematics with the width of the 'eight' corresponding to the extent of plunging can plausibly be advantageous for aerodynamic reasons. Hence the focus of this work has been idealized wing tip kinematics of that type, so that the results are practical to implement, but scientifically relevant both for engineers and biologists.

4 Presentation of Key Aspects of Controller Design

4.1 Model of Slender Body for Shape Control

Aeronautical and animalopter structures are continuous systems with spatially distributed dynamic properties. General mathematical model of such structures has the form of boundary value problem:

$$Aw = F, \quad w \in \Omega \tag{1}$$

$$B_j w\big|_{\partial\Omega} = g_j , \qquad j = 1,...,s \tag{2}$$

where: A – nonlinear, nonsteady differential operator, w – state variable; F – external loads, B_j – boundary value operator; g_j –functions defining the boundary conditions.
Such a general description is useful for problem formulation but it must be precised and simplified for obtaining useful results.
The standard model for elongated structures (such as airplane or animal wings) is a one dimension beam, described in the lack of damping by partial differential equation:

$$\mu(x)\frac{\partial^2 w}{\partial t^2} + \frac{\partial^2}{\partial x^2}\left[EI(x)\frac{\partial^2 w}{\partial x^2}\right] = P_z(x,t) \tag{3}$$

where $w(x,t)$ - beam deflection; μ - mass distribution along the span, $EI(x)$ - bending stiffness distribution along the beam span, $P_z(x,t)$ - external load distribution, t - time, x - spatial variable.
To complete the model the boundary conditions must be added to (3). For a cantilever model they take the form:

$$\begin{aligned} w(0,t) = 0, \quad & \frac{\partial w(0,t)}{\partial x} = 0 \\ \frac{\partial^2 w(l,t)}{\partial x^2} = 0, \quad & \frac{\partial^3 w(l,t)}{\partial x^3} = 0 \end{aligned} \tag{4}$$

where l is the beam length.
As the control theory for continuous systems is not sufficiently developed for direct applications, a discretization for continuous models is applied, usually by using the Galerkin method. In this method, the resulting aeroelastic displacements at any time are expressed as a function of a finite set of selected modes:

$$w(x,t) = \sum_{i=1}^{N} \varphi_i(x)\, q_i(t) \tag{5}$$

where: $\varphi_i(x)$ - coupled mode shapes for all deformations beam eigenmodes; $q_i(t)$ - normal coordinates.

After discretization the final matrix form of the aeroelastic equations of motion is

$$\mathbf{M}\,\ddot{\mathbf{q}} + \mathbf{K}\,\mathbf{q} = \mathbf{F}(t) \tag{6}$$

where: **M** - matrix of generalised masses:

$$M_j = \int_0^l \boldsymbol{\varphi}_j^2\,\boldsymbol{\mu}\,dx \tag{7}$$

K - matrix of generalised stiffness:

$$K_j = M_j\,\boldsymbol{\omega}_j^2 \tag{8}$$

and **F** - vector of generalised forces

$$F_j(t) = \int_0^l P_z(x,t)\,\boldsymbol{\varphi}_j\,dx \tag{9}$$

This technique may be applied to more complex systems

4.2 Control system design

The active control approach in this study is based on the deterministic linear optimal regulator problem. Results for this full state feedback controller are used as baseline against which other controllers are evaluated [11].

We present first the standard feedback design methodology. For control application the system (4) is transformed to a system of linear, first order differential equations in state and control variables:

$$\dot{\mathbf{x}} = \mathbf{A}\mathbf{x} + \mathbf{B}\mathbf{u} \tag{10}$$

$$\mathbf{y} = \mathbf{C}\mathbf{x} \tag{11}$$

where $\mathbf{x}(n\times 1)$ - vector of state variables, $\mathbf{u}(r\times 1)$ - vector of control variables, $\mathbf{y}(m\times 1)$ - the vector of system outputs, and **A**, **B** and **C** are state, control and outputs constant matrices of appropriate dimensions.

The objective is now to find control vector **u** that is the control input to the FMAV wings. Control system design is described as minimisation of *performance index* (called sometimes the *quadratic cost function*) in the form:

$$I = \tfrac{1}{2}\int_0^\infty \left(\mathbf{x}^T\mathbf{Q}\mathbf{x} + \mathbf{u}^T\mathbf{R}\mathbf{u}\right)dt \tag{12}$$

where $\mathbf{Q}(n\times n)$ is non-negative and $\mathbf{R}(m\times m)$ is positive definite symmetric weighting matrix. Applying calculus of variations for minimisation of performance index (12), the feedback control law is obtained in the form:

$$\mathbf{u}(t) = -\mathbf{R}^{-1}\mathbf{B}^T\mathbf{S}\mathbf{x}(t) \tag{13}$$

A constant, positive-definite symmetric matrix **S** in the feedback gain matrix is obtained as a solution of matrix algebraic Riccati equation:

$$\mathbf{S}\mathbf{B}\mathbf{R}^{-1}\mathbf{B}^T\mathbf{S} - \mathbf{S}\mathbf{A} - \mathbf{A}^T\mathbf{S} - \mathbf{C}^T\mathbf{Q}\mathbf{C} = 0 \tag{14}$$

Generally solution of Eq. (14) requires sophisticated numerical methods.

The resulting closed-loop dynamics equation is then defined as:

$$\dot{\mathbf{x}} = \mathbf{L}\mathbf{x}, \quad \mathbf{L} = \mathbf{A} + \mathbf{B}\mathbf{F} \tag{15}$$

where the feedback control matrix has the form:

$$\mathbf{F} = -\mathbf{R}^{-1}\mathbf{B}^T\mathbf{S} \tag{16}$$

For a controllable system such a solution yields to a stable closed-loop system, i.e. the eigenvalues $\boldsymbol{\lambda}_j(\mathbf{L})$, $j = 1,\ldots,n$ of **L**, and

$$\mathrm{Re}\,\boldsymbol{\lambda}_j(\mathbf{L}) < 0 \tag{17}$$

lie in left-half plane of the complex plane.

This method is referred as the *linear regulator problem*. By this method systems may be stabilised in the range of parameters essential for the system application.

Based upon the assumption of a model with "fixed" C_m, it is possible to devise a set of the angle of attack α, the sideslip-angle β.

Let us assume that at initial time, prior to the beginning of a manoeuvre, the wind reference frame coincides with the local horizontal reference frame. This situation may correspond to a steady-state level flight.

We want to guide the animalopter from a given initial state to a given terminal state in minimum time.

4.3 Control via Smart Structure Technology – MAVs vs. Insects

Recent application of piezoelectric (PZT) materials for structural vibration suppression has added new dimensions to the control system. Because of the direct and converse effects of PZT materials, the dream of an smart structure, which is defined as a structure with the integrated sensor/actuator system, is beginning to be realized. Emerging "smart structure technology" is widely investigated for application to enhance rotorcraft performance[7]. Application of smart structures to shape control for adapting rotor behavior to surrounding conditions and to a flight regime is a new concept giving prospect of combination into one mechanism primary and additional controls of a helicopter rotor. Changing of the blade cross section shape using different active materials is considered. The idea of controlling blade shape can be put into practice by using of smart composite in the form of either fibers or rods embedded inside the blades. Active composites are offered now by some manufacturers and are being used to change the blade structure.

The facts described above form the background for undertaking the study in which a model of elastic blade is modified by application of actively controlled elements or fibers.

In the field of biomechanics, the flight performance of insects has been studied extensively. The studies show that not only do some insects actively generate torsional motion, but also they passively change the torsional angle of their wings by inertial and aerodynamic forces resulting from the beating motion. Such passive changes in the torsional angle and wing shape are important in the flight of insects. For example bumblebee wings do not make simple up and down movements, but in the course of each cycle also move backwards and forwards to some extent. The plane in which the wings vibrate relative to the bumblebee's body is called the stroke plane. During the beating motion, the forewing and hindwing of a bumblebee are in the same plane, so that the wing moves as a single wing. It is possible to measure the flapping angle, lag angle and torsional angle of this single wing, and it is possible digitizing the distorted projected lines on the image of the CCD camera, and got the spatial coordinates of the wing with respect to each distorted projected line. As the flapping angle increases, the projected line spacing on the wing changes. To ensure that the torsional angle and torsional deformation measured are at the same section with respect to different flapping angle, it is possible to calculate them by using an interpolation method.

Figure 10 shows the interpolation method. Consider arc AB distorted projected line. It is possible to divide line A_1B_1 that joins leading edge A_1 and tailing edge B_1 into 12 equality parts: D_1 , D_2 , . . D_{12}, and then made a group of plane, each passes through D_i , i is1, 2, . . . ,12, and perpendicular to line AB. These planes cross with arc AB at point E_1 , E_2 , . . . E_{12} . Similarly, we get M_1 , M_2 , . . . ,M_{12} with respect to arc AB . To get the torsional deformamtion at the section AB, A is the point at leading edge and between points A_1 and A_2, we make a plane p that passes through A, perpendicular to n leading edge and crosses with tailing edge at point B. Lines E_1M_1 , E_2M_2 , . . .$E_{12}M_{12}$ cross with plane at points N_1, N_2 , . . . N_{12}. Then the torsional deformation can be expressed by arc AN_1, N_1N_2, . . .$N_{12}B$ as shown in Figure 10.

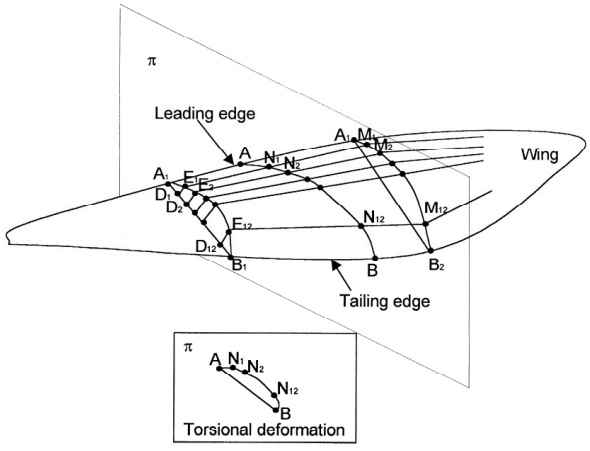

Fig. 10 Deformation of entomopter wing [29]

4.4 Control via Multiwire Wing Structure – Flying Insects Morphology Overview

Another approach to shape wing control, named by us "control via multiwire wing structure", is presented in Ref. [14, 15]. The chief function of the veins is to provide support for the wing and

act as cantilever beams and elastically transmit force (see Fig. 10). A great variety of often-complicated venation schemes occurs in insects. However, selecting the structurally important spars and ignoring those with less obvious mechanical functions can simplify the wing design for an MAV. Such an efficient pattern is observed in flies, which are excellent flyers. The occurrence of one or more supporting veins near the leading edge of the wing allows to modify the angle of attack during flapping cycle by actively twisting the joints. This action is performed against the aerodynamic and inertial moments, and the torsional elasticity of the wing base.

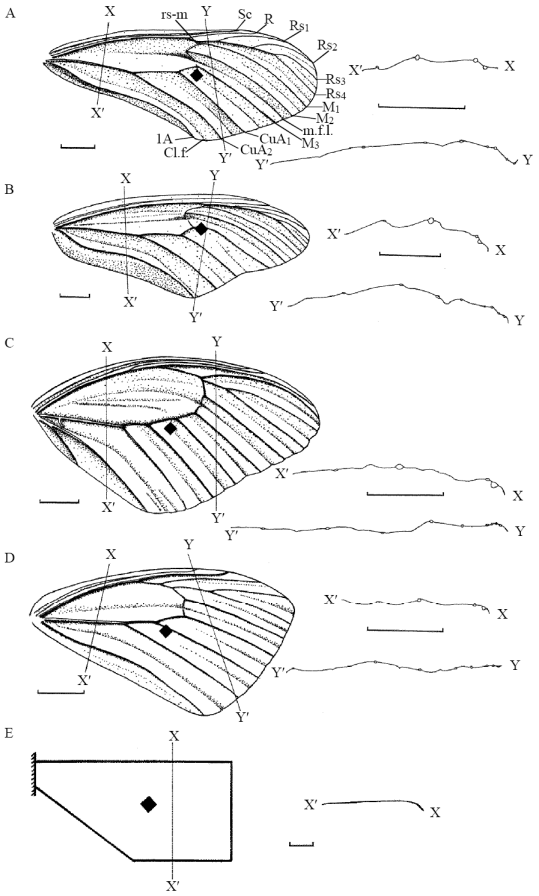

Fig. 11 (A–D). Plans and two sections of the forewings of the butterflies (A) *Heliconius charitonia*; (B) *Dryas julia*; (C) *Papilio polytes*; (D) *Pieris brassicae*; (E) Plan and cross section of paper model wing. (Symbols shown in (A) means: m.f.l. - median flexion line; cl.f. - claval furrow; Sc - subcosta; R - radius; Rs1,2,3,4 - branches of radial sector; M1,2,3 - branches of media; CuA1,2 - branches of anterior cubitus; 1A - first anal vein. rs-m - cross-vein linking Rs and M). X–X9, Y–Y9 show the positions of the transverse sections so labeled. Scale bars represent 5mm. (cf. Ref. [29]).

As a cantilever beam, the wing needs to accept the shifting pattern of bending and twisting forces without structural failure. Since wings accelerate and decelerate, these forces include a significant inertial component. Considerable deformability of wings allows withstanding these loadings over thousands of flapping cycles throughout the insect's life. Also, controlled changes of wing shape during the flapping cycle is essential to develop adequate thrust and lift. Finally, having the center of mass of the wing behind the torsional axis helps the wing to twist at the end of each half-stroke (see ref [14]).

The functional morphology of butterfly wings will be treated in detail in many papers (see for example papers by R. J. Wootton, in preparation). Briefly, forewings and hindwings differ in size and shape and in some details of venation. They are not physically coupled in flight, but overlap appreciably, and normally beat in phase, acting as a single pair of aerofoils. However, they are capable of separating slightly, particularly during glides (Betts and Wootton, 1988), and far greater separations can occur momentarily (S. J. Bunker and R. J. Wootton, unpublished observations from high-speed film). We are concerned here only with the forewing (Figure 11). This is supported by a framework of thin-walled tubular veins, which taper to the margin. With the exception of the most anterior vein (subcosta, Sc) and the most posterior veins (the one or two anals), the framework consists of a large, often more or less elliptical, cell and of the distal extension of the radius (R), and the branches of the radial sector (Rs), the media (M) and the anterior cubitus (CuA), which radiate from the cell to the leading edge, the wing-tip and the outer trailing edge. The veins forming and emerging from this cell all lie in nearly the same plane. Immediately adjacent to the radius lies the subcosta, a stout vein whose anterior edge lies significantly below the plane of the rest of the wing. In front of this is a band of membrane, with a slightly thickened margin which forms the leading edge. There is no costal vein. The wing has two fully developed flexion lines, which pass from the axilla to the margin. The more anterior, a narrow band of flexible cuticle, bisects the elliptical cell, crosses its apex at a flexible

section of the cross-vein-like base either of M2+3 or of M3, and runs to the outer posterior margin. This line, which originates between the bases of R+Rs and CuA, allows relative pronation and supination of the anterior section of the wing, creating and eliminating camber. The second flexion line is the claval furrow, which lies in front of the more anterior anal vein, and allows the wing to be pronated and supinated relative to the narrow posterior clavus and to the hindwing. Neither of these flexion lines appears to be in a position to influence distal torsion and, as we shall see, the asymmetric twisting behaviour of the wings persists when the lines are immobilised at the axilla. Its cause must lie elsewhere. The most probable candidate appears to be the cambered cross section. The wing relief of butterflies has attracted little attention. It is most obvious in the membrane, which has deep grooves between and parallel to most of the longitudinal veins. The local effects of these grooves on wing section in flight have been discussed by Brackenbury (1991). In many – perhaps all – butterflies, however, the anterior strip of the forewing, immediately behind the leading edge, is deflected ventrally. The extent of the deflection, and the location of the posterior boundary of the strip, vary with species (Figure 11). Of the four species studied here, the downward curve is least marked in *Pieris brassicae*, being confined to the basal area anterior to R, which forms its posterior boundary (Fig. ``D). In *Papilio polytes*, the boundary ridge follows the common stem of R and Rs, continues along Rs1, which lies close behind R and Sc, and runs to the wingtip along Rs2, which has curved anteriorly to lie adjacent to Rs1 (Fig. 11C). The anterior strip is therefore narrow, but the camber is steep. In the Heliconiinae *Heliconius charitonia* and *Dryas julia* the posterior boundary ridge of the downwardly deflected strip follows R+Rs, Rs1+2+3 and Rs2+3, and the strip is, therefore, relatively broader than in *Papilio polytes*. The anterior camber is clear in both species and particularly marked in the longer-winged *Dryas Julia* (Figure 11 A, B).

The dorsoventrally asymmetric flexural rigidity of thin cambered plates, including insect wings, has already been noted in many papers (see for example Wootton, 1981; Betts, 1986). A cantilevered plate, point-loaded through the shear centre of its cross section from the concave side, is far more rigid than if loaded from the convex side. In the former case, the force tends to increase the camber, and hence the second moment of area of the cross section and the overall rigidity of the plate. If a thin cantilevered plate is loaded at a point some distance from the shear centre of its cross section, so that it is both bent and twisted, it again deforms asymmetrically according to the direction of application of the force. A point force applied to the concave side twists the plate, but this is rapidly arrested. A similar force to the convex side, however, causes a much greater deflection: the plate twists freely and tends to flex along an oblique line running anterodistally from the base of the posterior edge. A insect (for example butterfly) forewing can be modelled in its entirety as a plate of this kind, or its ventrally curved anterior margin can be regarded as a narrow cambered plate with the rest of the wing attached along its posterior edge. If the centre of pressure lies behind the shear centre of the plate's cross section, its effect in each model will be essentially similar.

Ennos (1988*a*), examining wing torsion in three species of Diptera, used a torsion balance that applied a couple to the wing-tip, and so loaded the wing in pure torsion. He, too, found that the wings were more compliant to supinatory than to pronatory torques, but did not explain the mechanism. The balance used in the present work measures the total deflection of the wing and so allows both torsion and bending, which clearly interact. Since the wing bases were immobilised in the experiments, it is clear that the observed difference in resistance to pronating and supinating torques is a property of the wings beyond their axillae. In the flying insect, this effect would be superimposed on the active pronation and supination of which the insect is capable and would allow the distal part of the wing to twist disproportionally in the upstroke, so rotating the net aerodynamic force vector in the direction of greater weight support and permitting slow flight and manoeuvring at low speeds. The experimental results from the

paper model, together with a great deal of unpublished, non-quantitative experience of manipulating various other models, support the contention that the curved leading edge section is, by itself, capable of producing this observed asymmetric rigidity. Modelling the wing in this way, we are treating it as a thin curved plate. It is important to examine the ways in which the real forewing differs from this simple model and how the differences might be expected to affect functioning.

The curved plate is made of a single material, of uniform thickness, whose properties are constant throughout. It has appreciable stiffness in compression, as well as in tension and shear. In contrast, the wing is a framework of fairly rigid tubes, varying in section and perhaps in material properties both along their length and between individual tubes, linked by a membrane whose thickness and properties vary around the wing, but which is probably only significantly stiff in compression in the thickened band along the leading edge. Two implications of this difference require comment. First, a force applied to the uniform plate would be transmitted through the structure by the material as a whole, whereas a force applied to the wing would be transmitted variously as tension or compression by the veins, but only as tension by the membrane. The precise distribution of forces induced in a real wing by a distributed aerodynamic load or by a point load close to the presumed centre of aerodynamic pressure is at present impossible to determine, but it seems clear that torque would be transmitted to the leading edge spar – Sc, R and the branches of Rs, and the membrane anterior to and between them – primarily by the crossvein rs-m (Figure 8A) This would be levered up in pronation and down in supination by the applied force centred behind it. The spar, with its curved section, would deflect in much the same way as the anterior band of the uniform plate, and the wing-tip would similarly twist more easily in supination. Second, the curved plate deflects by bending as well as twisting. The leading edge spar of the real wing is stiffened by the veins, which might therefore interfere with the effect. This proves not to be the case; indeed, the veins may actually assist the mechanism.

5 MAV Mathematical Model

5.1 General Remarks

The dynamical description of a flexible structure must accurately represent all structural characteristics by relating dynamic responses at specific locations throughout the structure to forces acting on the system. Mathematically speaking, the motion of animals with distributed elastic parts can be described by a set of ordinary differential equations for the rotational motion of a given reference frame, and a set of partial differential equations for the elastic motion relative to that frame. Such a system of differential equations is known as a *hybrid dynamical system.*

Often, in the aerospace industry, the analysis of unmanned spacecraft with flexible appendages begins with the assumption that the attitude and the vibrational motions of the spacecraft are uncoupled. Such analyses are performed for bounding the spacecraft jitter due to instrument disturbances.

For our study the motion of the animalopter will be represented in the most general way by the differential equations (18).

$$\dot{\mathbf{x}} = \mathrm{f}(\mathbf{x}, \mathbf{u}) \qquad (18)$$

where : $\mathbf{x}$ – is the state vector, $\mathbf{u}$ – is the control vector. For rigid MAV

$\mathbf{x}=[U, V, W, P, Q, R, \Theta, \Phi, \Psi]^T$

where U, V, W are the forward, side, and yawing velocities of the animalopter; P, Q, R are the angular velocities, roll, pitch, and yaw, Θ, Φ, and Ψ are roll and pitch angels (Figure 6). In Ref. [5, 7] vector $\mathbf{u}$ was taken in the form $\mathbf{u} = [\delta, \gamma, \omega, \lambda]^T$ where: γ - feathering angle of wings, δ - flapping angle of wings, ω - frequency of wing motion respect to the body, λ - phase shifting between feathering and flapping

We propose to derive the system equations of motion by means of Lagrange's procedure.

$$\frac{d}{dt}\frac{\partial T}{\partial \dot{\mathbf{q}}} - \frac{\partial T}{\partial \mathbf{q}} + \frac{\partial (U+V)}{\partial \mathbf{q}} = \mathbf{F}_q \qquad (19)$$

where T is the kinetic energy, U is the strain energy, U is the gravitational energy, F_q is the vector of nonpotential external forces, and $\boldsymbol{q}$ is the vector of generalized coordinates.

5.2 Systems of Coordinates

An important ingredient in the treatment of coupled wing/body problems is a clear definition of the coordinate systems, because various systems will be used (Figure 12). It is worth noting that problems involving flight control systems are generally related to events which do not persist: the dynamic situation being considered rarely lasts for more than a few minutes. Consequently, a more convenient *inertial* reference frame is a tropocentric coordinate system, i. e. one whose origin is regarded as being "fixed" at the center of the Earth: the *Earth* or *gravitational* axis system $\mathcal{G}$ (not shown in Figure 12). It is used primarily as a reference system to express gravitational effects, altitude, horizontal distance, and the MAV orientation.

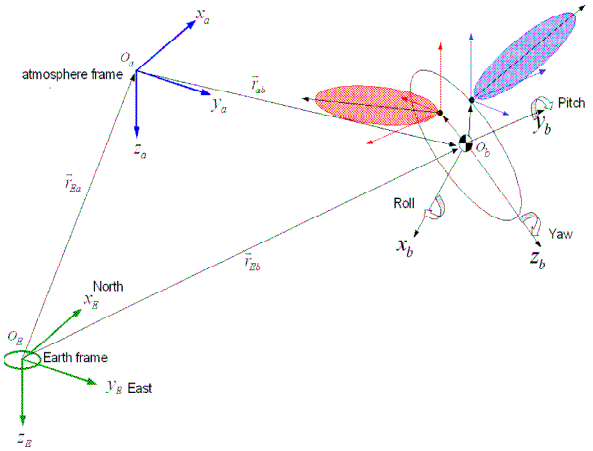

Fig. 12 System of Cordinates (cf. Agrawal and Khan [1, 2])

The next one is the system fixed to MAV body, rotating with angular velocity $\boldsymbol{\Omega} = [P, Q, R]^T$; P, Q, R are the *roll*, *pitch*, and *yaw* angular velocities. The axes of this system are denoted as x, y, z with the versors $\mathbf{e}_x$, $\mathbf{e}_y$, $\mathbf{e}_z$. The relative position of the system x, y, z attached to the animal is described by Euler angles Φ, Θ and Φ, while the relative position of the system x_a y_a z_a attached to the airflow by the angle of attack α and slip angle β. The relationship between the Euler angles and angular velocity has the traditional form:

$$\begin{aligned} P &= \dot{\Phi} - \dot{\Psi}\sin\Theta \\ Q &= \dot{\Theta}\cos\Phi + \dot{\Psi}\cos\Theta\sin\Phi \\ R &= -\dot{\Theta}\sin\Phi + \dot{\Psi}\cos\Theta\cos\Phi \end{aligned} \qquad (20)$$

Next we define a set of wing axes ξ_j, η_j and ζ_j (j=1,2), as the principal axes for the wings in the undeformed configuration with the origins at the wing roots. The sets ξ_j, η_j and ζ_j, provide the reference frames for measuring deformations whereas the set xyz is more convenient for describing the over-all motion.

5.3 Physical Model of Animalopter

The animalopter model used for this study includes six-degree-of-freedom "fuselage" dynamics. The wings are modeled structurally as a Bernoulli-Euler beam with inertially coupled bending and twisting motions. The essential features of this model are described below:

- The "fuselage" may assume large rigid body displacements with respect to the fixed axis system.
- The wing is cantilevered beam;
- Wing material has linear isotropy and Hooke's law is applicable;
- The curvature and deflections of the deformed wing are small;
- The wing elastic axis (E. A) forms a straight line;
- The wing can bend in two perpendicular directions and twist around E. A.;
- The wing cross-section (airfoil) do not deform, nor warp.
- The tension loads are included.

5.4 Kinetic Energy Contributions

The total kinetic energy is defined by the formula:

$$T = \frac{1}{2}\iiint_{\tau} \rho \frac{d\mathbf{R}}{dt}\cdot\frac{d\mathbf{R}}{dt}\,d\tau \qquad (21)$$

where ρ is the mass per unit volume, assumed invariant with respect to time, and a position

vector **R** is referred to an orthogonal inertial axis system $\mathcal{I}$. When the origin of the *x-y-z* coordinate system is taken at the center of gravity of the animalopter, then we have :

$$\mathbf{R} = \mathbf{R}_C + \mathbf{R}_l + \mathbf{r} \tag{22}$$

where $\mathbf{R}_C$ is the position vector to the center of gravity, $\mathbf{R}_l$ is the *local* position vector to the wing roots, and ***r*** is a position vector of a particle in the ξ_j, η_j and ζ_j (j=1,2), -axis system.

Using assumption that the wing cross-section do not deform nor warp, the position vector ***r*** of a wingpoint after deformation is given as (Fig. 12)

$$\mathbf{r} = \mathbf{r}_0 + \mathbf{u} + \mathbf{T}\cdot\boldsymbol{\rho} \tag{23}$$

$$\begin{aligned} \mathbf{r}_0 &= \begin{bmatrix} \xi_j & 0 & 0 \end{bmatrix}^T \\ \mathbf{u} &= \begin{bmatrix} u & v & w \end{bmatrix}^T \\ \boldsymbol{\rho} &= \begin{bmatrix} \xi & \eta & \zeta \end{bmatrix}^T \end{aligned} \tag{24}$$

$$\mathbf{T} = \begin{bmatrix} \cos\varsigma\cos\beta & \cos\varsigma\sin\beta\sin\phi - \sin\varsigma\cos\phi & -\cos\varsigma\sin\beta\cos\phi - \sin\varsigma\sin\phi \\ \sin\varsigma\cos\beta & \cos\varsigma\cos\phi + \sin\varsigma\sin\beta\sin\phi & \cos\varsigma\sin\phi - \sin\varsigma\sin\beta\cos\phi \\ \sin\beta & -\cos\beta\sin\phi & \cos\beta\cos\phi \end{bmatrix} \tag{25}$$

The position of an arbitrary point after the wing has deformed is given by (ξ_j, η_j, ζ_j) j=1,2 where

$$\begin{aligned} \xi_j &= \xi - v'(\eta\cos\varphi - \zeta\sin\varphi) + \\ &\quad - w'(\eta\sin\varphi + \zeta\cos\varphi) \\ \eta_j &= v + \eta\cos\varphi - \zeta\sin\varphi \\ \zeta_j &= w + \eta\sin\varphi + \zeta\cos\varphi \end{aligned} \tag{26}$$

The velocity of this point of the wing with respect the inertial frame $\mathcal{I}$ is

$$\mathbf{V} = \frac{\delta\mathbf{r}}{\delta t} + \boldsymbol{\Omega}\times\mathbf{r} \tag{27}$$

where $\delta/\delta t$ is the derivative in the rotating frame $\mathcal{R}$, and

$$\mathbf{r} = \xi_j\mathbf{i} + \eta_j\mathbf{j} + \zeta_j\mathbf{k} \tag{28}$$

The term **Ω** x **r** is the velocity contributed by the rotating coordinate system. The velocity in the rotating frame $\mathcal{R}$ is:

$$\frac{\delta\mathbf{r}}{\delta t} = \dot{\xi}_j\mathbf{i} + \dot{\eta}_j\mathbf{j} + \dot{\zeta}_j\mathbf{k} \tag{29}$$

In view of above-mentioned, the total kinetic energy can be written as:

$$T = \tfrac{1}{2}mV_C^2 + T_{rot} + T_{coup} + T_{vib} \tag{30}$$

where m is the total mass of the animalopter

$$T_{rot} = \frac{1}{2}\boldsymbol{\Omega}^T\mathbf{J}\boldsymbol{\Omega} \tag{31}$$

where ***J*** is the inertial tensor

$$\mathbf{J} = \begin{bmatrix} I_x & -D_{xy} & -D_{xz} \\ -D_{xy} & I_y & -D_{yz} \\ -D_{xz} & -D_{yz} & I_z \end{bmatrix} \tag{32}$$

Two additional terms T_{coup} and T_{vib} in the formula (30), are nontrivial one, and be specified later.

5.5 Strain Energy Contributions

In the presented approach, the crucial point of derivation expressions describing elastic loads (see Figure 16) is formulation of the potential energy U of system elastic deformation. The general form of the elastic energy formulae can be expressed as

$$U = \frac{1}{2}\int_{\tau}\boldsymbol{\sigma}_{kl}\boldsymbol{\varepsilon}_{kl}d\boldsymbol{\tau}, \quad k,l = 1,2,3 \tag{33}$$

where σ_{kl} and ε_{kl} are stress and strain tensor components, respectively. For slender body, such like animalopter wing, formula (33) can be simplified to the form:

$$U = \frac{1}{2}\int_0^b\iint_A\left(\sigma_{11}\varepsilon_{11} + 2\sigma_{12}\varepsilon_{12} + 2\sigma_{13}\varepsilon_{13}\right)dAd\xi \tag{34}$$

where b is the wing length and A is the area of the wing cross section. Using Hooke law:

$$\sigma_{11} = E\varepsilon_{11}, \quad \sigma_{12} = G\varepsilon_{12}, \quad \sigma_{13} = G\varepsilon_{13} \tag{35}$$

where E, and G are Young's modulus and shear

modulus, respectively.
Formula (33) is transferred to the form:

$$U = \frac{1}{2}\int_0^b \int_A \left(E\varepsilon_{11}^2 + 2G(\varepsilon_{12}^2 + \varepsilon_{13}^2) \right) dA d\xi \tag{35}$$

An elastic axis of the undeformed wing coincides with the ξ-axis
Using Eq. 5 taken from Ref. 10 describing the relations between displacements we can obtain the formulae:

$$\begin{aligned} \varepsilon_{11} &= u' - (\eta\cos\varphi + \varsigma\sin\varphi)v'' + \\ &+ (\eta\sin\varphi - \varsigma\cos\varphi)w'' \end{aligned} \tag{37}$$

$$\varepsilon_{12} = \frac{1}{2}\varsigma\phi', \quad \varepsilon_{13} = -\frac{1}{2}\eta\phi' \tag{38}$$

From (37) the strain component u' is eliminated applying condition [4]

$$t(\xi) = \int_A \sigma_{11} dA \tag{39}$$

where $t(\xi)$ is the tension force in a wing section. Introducing the Hook law (35) into (37) and then (37) into (39) we obtain:

$$\begin{aligned} u' &= \varepsilon_T + (\eta_T\cos\varphi + \varsigma_T\sin\varphi)v'' + \\ &+ (-\eta_T\sin\varphi + \varsigma_T\cos\varphi)w'' \end{aligned} \tag{40}$$

where

$$\varepsilon_T = \frac{t_a(x)}{A_E}, \quad A_E = \int_A E dA \tag{41}$$

$$\eta_T = \frac{1}{A_E}\int_A E\eta dA, \quad \varsigma_T = \frac{1}{A_E}\int_A E\varsigma dA \tag{42}$$

Inserting (40) into (37) we obtain:

$$\begin{aligned} \varepsilon_{11} &= \varepsilon_T - \begin{bmatrix} (\eta-\eta_T)\cos\varphi + \\ +(\zeta-\zeta_T)\sin\varphi \end{bmatrix} v'' - \\ &- \left[(\eta-\eta_T)\sin\varphi - (\zeta-\zeta_T)\cos\varphi \right] w'' \end{aligned} \tag{43}$$

Formula (43) expresses the strain in any point of the wing cross section.

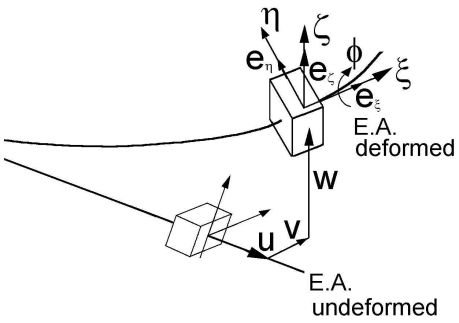

Fig. 13 Deformation of wing elastic axis (E. A)

The potential energy U is obtained from (34) including the strains given by (38) and (43).
To obtain the animalopter model in ordinary differential equations form, the Galerkin [11] method may be applied. Thus the elastic displacements of the wings are decomposed as:

$$v(\boldsymbol{\xi}, t) = \sum_{i=1}^{N_v} \boldsymbol{\eta}_i(\boldsymbol{\xi})\, q_i(t) \tag{44}$$

$$w(\boldsymbol{\xi}, t) = \sum_{i=1}^{N_v+N_w} \boldsymbol{\eta}_i(\boldsymbol{\xi})\, q_i(t) \tag{45}$$

$$\boldsymbol{\phi}(\boldsymbol{\xi}, t) = \sum_{i=1}^{N_v+N_w+N_\phi} \boldsymbol{\eta}_i(\boldsymbol{\xi})\, q_i(t) \tag{46}$$

where N_V, N_W, and N_ϕ are numbers of modes for in-plane, out-of-plane, and feathering modes, respectively.

6. Formulation of manoeuvring dynamics and nonlinear control issues

Consider manoeuvring MAV according to the prescribed configuration vector:

$$\mathbf{x}_d = [\varphi_d(t), \theta_d(t), \psi_d(t); \xi_1^d(t), \ldots, \xi_k^d(t)]^T \tag{47}$$

where $\varphi_d(t), \theta_d(t), \psi_d(t)$ and $\boldsymbol{\xi}_{\boldsymbol{\kappa}}^d(t), \boldsymbol{\kappa} = 1, \ldots, k$ are the desired attitude and elastic behaviour. Introducing the configuration error vector:

$$\mathbf{e} = \mathbf{x} - \mathbf{x}_d \tag{47}$$

the state-space equation of motion can be presented in the terms of $\mathbf{e}$ and $\mathbf{x}_d$.

If $\varphi_d(t), \theta_d(t)$ and $\psi_d(t)$ are explicit prescribed function of time, a tracking problem for the animalopter will be obtained.

Quite a few reasons exist for why flapping flight could benefit greatly from an active, i.e., closed loop, control system. Open loop flow control performs well when the operating conditions are carefully restricted to the range within which the control mechanisms were designed. But outside the lab the operating environment can vary considerably from one instant to the next due to environmental factors such as a gust or wind or even due to mechanical damage to the wings themselves. Therefore, an active control system is needed to compensate for a wide range of flight conditions. Also, specifications for increased maneuverability call for an adaptive control technology that can intelligently alter the wing shape in order to generate adequate lift to meet the lowered wing loading requirement. Additionally, mechanical wings currently cannot effectively imitate the full range of motion and control displayed by natural wings and so it is no surprise that mechanical wings suffer in terms of performance compared to their biological counterparts. There are no muscles, feathers, or bone structure in mechanical wings comparable to those found in bird or bat wings. Active flow control therefore is a key component in closing the performance gap between the two without having to fully mimic the biological flapping motion, and hence reducing the mechanical complexity of the system. Essentially, satisfactory wing performance beyond the limited and narrow design range drives the demand for active flow control of flapping wings. The major challenges of animalopter control system development largely center on an appropriate control system which can properly handle the complexity of the aeroelastic problem at hand. Previous sections have described the difficulties in aeroelastic analysis of the flexible flapping wing system. In the parlance of dynamic control engineers, the ‘‘plant’’, i.e., the flapping wing MSV complete with sensors and actuators, is a highly nonlinear system and there seems to be no linear control law or even an appropriate linear approximation. An active wing will, by definition, have many variable parameters, e.g., camber, stiffness distribution, twist, kinematical limitations, and this leads to a large state space for optimization. For example, if only 10 actuators with 5 states apiece are on the wing, then almost 10 million combinations are possible! This staggering number of states creates quite an optimization and control problem.

This section starts with an overview of closed loop linear control schemes. Then it quickly moves to nontraditional control algorithms such as genetic algorithms and neural nets and reviews their past application in a variety of active flow control experiments. Next, the Gur Game, a new nonlinear control algorithm, will be described. The Gur Game is especially appropriate for a distributed system of actuators operating in a nonlinear system. Some results using this new controller in optimizing wing kinematics then follows.

6.1 Closed Loop Control of Separated Flows

Linear optimal control of flutter comprises the vast majority of work on closed loop separated flow control. This was largely due to the ease of analytically modeling and predicting linear systems with the limited computing technology available at the time. If the systems were inherently nonlinear, “reasonable” linearizing assumptions were made for either the fluid or structural mechanics models. While this approach has worked satisfactorily for many years, the recent requirements of supermaneuverability and the advent of active materials (particularly piezoelectric transducers and MEMS sensors and actuators) now invalidate the old assumptions of attached flow, small wing deformations, and static material properties. Fortunately, the explosive growth of computing power has made possible the exploration of more computationally intensive control algorithms, such as genetic algorithms and artificial neural networks (ANNs). First, however, we start with linear control algorithms.

6.2 Linear Quadratic (LQ) Controllers

The vast majority of closed loop control systems apply linear optimal control theory in order to produce a computable solution in terms of gain and phase margins. The use of LQ and linear quadratic Gaussian (LQG) controllers for active flutter suppression has a relatively long history. Theoretical work by Edwards et al. [31 considered an extension to the standard computation of flutter whereby the generalized unsteady aerodynamic loading was represented by a rational transform instead of a simple harmonic function. However, the transforms were still in the Laplace splane and hence the loading was still linear. Newsom [32] followed the same path when he employed a Pade approximation to derive a deterministic LQ control law for flutter suppression using a trailing edge flap. Numerical simulations showed as much as 50% increase the dynamic flutter pressure, but again the model linearized aerodynamic loading with relatively small wing deformations.

Experimentally, Mahesh et al. [33]studied LQG control on a swept back wing with an active control surface. After calculating a high order LQG controller using linear aeroelastic theory with assumed simple harmonic steady-state wing motion, the group compared the use of residualization and frequency response matching to achieve lower order controllers. They found improvement in performance (adequate gain and phase margins), but it was only at one specific Mach number and they noted gain scheduling may be required for a range of Mach numbers. Mukhopadhyay [34] published results using LQG controller on a flexible wing with a trailing edge flap actuator and surface mounted accelerometers. After control law synthesis and order reduction of the controller, the closed loop controller increased the flutter pressure by 23% over the uncontrolled case. But he noted that discrepancies arose between the analytical and experimental frequency response for the actuator, which he attributed to the approximate modeling of the unsteady aerodynamics using attached flow when in fact, the flow may have separated. This points out the need for a viscous aerodynamic model that accounts for flow separation when dealing with flutter simulations. Finally, Lazarus et al.[34] used a LQG controller in conjunction with piezoelectric actuators to effect a change in flutter speed purely through changing the structural properties (namely the strain characteristics) of the wing. The result was an increase in flutter speed of 11%. This showed that a flap actuator was not needed to change the aerodynamic performance or flutter characteristics, but instead simple strain actuation could provide a means of extending the performance envelope.

6.3 Other Linear Controllers

Luton and Mook [36] conducted an interesting numerical study where they used linear feedback on the control of ailerons to suppress flutter on a nonlinear high aspect ratio wing undergoing large deflections. They employed unsteady vortex-lattice methods to model the flow, and so this model is not valid if the flow separates or if vortex bursting occurs. The simulation computed that the flutter divergence speed increased by almost 100%.

Frampton et al. [37] demonstrated the control of panel flutter with piezoelectric transducers, which acted as both sensors and actuators. Here they used linearized potential flow aerodynamics and calculated the response of a panel with an attached piezoelectric transducer mounted on the surface. The control law for the transducer used collocated direct rate feedback, in which a voltage input signal proportional to the sensed structural velocity was sent to the piezoelectric actuator. Stability was achieved for a limited range of transonic and supersonic flows, but they noted that actuator saturation limited the amount of which this system could be stabilized.

6.4 Proportional Integral Derivative Control

Gursul et al. [38] changed the sweep angle of the delta wing to control vortex breakdown location. An integral feedback controller sought to minimize the rms value of pressure fluctuations induced by the helical mode

instability found in vortex breakdown as a function of the sweep angle. This approach proved fruitful as the amplitude of the pressure fluctuation monotonically varies with the vortex breakdown location, thus making a simple first-order feedback control system possible. However, it is certainly not energetically efficient.

7 Results of Simulations – Hovering Control

In figures 14, 15 and 16 exemplary results of simulations of hovering stabilization are presented:

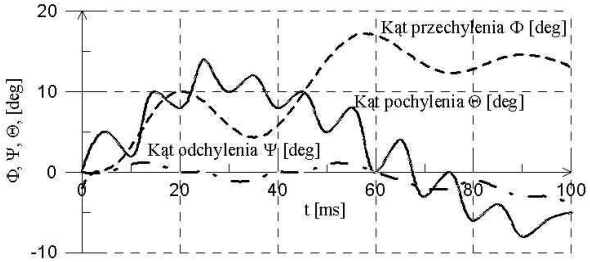

Fig. 14 Hovering stabilization. Angular position of Entomopter

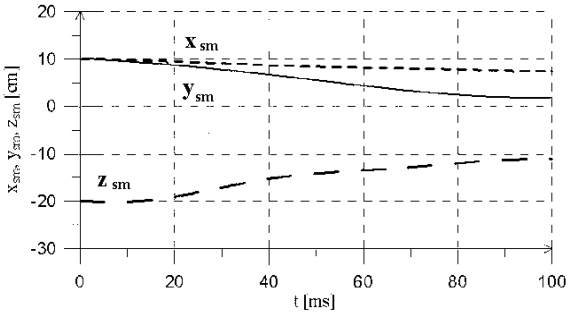

Fig. 15 Hovering stabilization. Position of centre of mass of Entomopter.

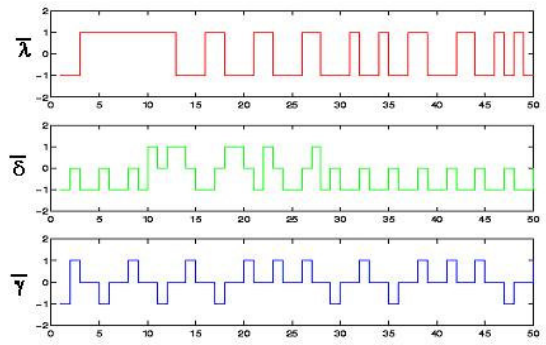

Fig. 16 Stabilization of hovering flight. Courses of control vectors (values of angles in relation to amplitudes of oscillations): $\overline{\lambda} = \lambda / \lambda_0$, $\overline{\delta} = \delta / \delta_0$, $\overline{\gamma} = \gamma / \gamma_0$

8 Summary

The MAVs development, apart from "theoretical" problems connected with modelling of their aerodynamics, flight and control dynamics also generates a lot of serious technical problems. One of those is the integrations of systems mounted inside of the apparatus. Because of small size of the cargo space of the MAV the distribution of the necessary devices, units and on-board sensors becomes an extremely serious problem. The conception used in "large" aeroplanes, consisting in filling the inside of the airframe with necessary instruments and then equipment – programme integration in this case is practically impossible.

Probably the most difficult element of the MAV to design is the system of flight control, which should by highly autonomous and should operate instantaneously. Relatively strong forces and moments caused by laminar flow (in entire flight range) act on the MAV. Moreover it is very difficult to foresee the conditions in which the flight will take place. Because of little mass and dimensions (moments of inertia) the effects of unstationariness of flow caused by gushes of the air and manoeuvres will significantly influence the aerodynamic loads of the MAV.

Acknowledgments

This work was funded by Ministry of Sciences and Higher Education of Republic of Poland as a Grant No. 4 T12C 023 30.

References

[1] Agrawal S. K,. Khan Z. A..; Force and Moment Characterization of Flapping Wings for Micro Air Vehicle Application; *American Controls Conference, Portland, Oregon*, 2005.

[2] Agrawal S. K., Khan Z. A..; Modeling And Simulation Of Flapping Wing Micro Air Vehicles , *ASME International Design Engineering Technical Conferences, Long Beach, California, USA,*, 2005.

[3] Azuma A, Masato O and Kunio Y.: Aerodynamic characteristics of wings at low Reynolds Numbers. *Fixed and flapping wings aerodynamics for micro air vehicle applications*, Ed T, J, Mueller, Progress in Astronautics and Aeoronautics, AIAA, Reston, 2001, pp 341-398.

[4] Azuma A.: *The biokinetics of flying and swimming*, Springer Verlag, Tokyo, 1998.

[5] Choromański P.: *Modeling and simulation of flying insect space detection system - in aspect of flapping wings Micro-Aerial-Vehicle (MAV) hovering flight stabilization*, M. Sc. dissertation, Faculty of Mechanical Engineering, Białystok University of Technology, Białystok, 2006 (In Polish).

[6] Deng X., Schenato L., and Sastry S.: Model identification and attitude control scheme for a micromechanical flying insect, *Proc. 7th Int. Conf. ICARCV*, Singapore, Dec. 2002, pp. 2112–2118.

[7] Dickinson M. H.: Directional sensitivity and mechanical coupling dynamics of campaniform sensilla during chordwise deformations of the fly wing, *J. Experimental Biology*, vol. 169, 1992, pp. 221–233.

[8] Dickinson M.H., J. Palka J.: Physiological properties, time of development, and central projection are correlated in the wing mechanoreceptors of Drosophila, *J. Neuroscience*, vol. 7, no. 12, 1987, pp. 4201–4208.

[9] Dickinson M.H.: Comparison of encoding properties of campaniform sensilla of the fly wing, *J. Experimental Biology*, vol. 151, 1990, pp. 245–261.

[10] Dudley R.: *The biomechanics of insect flight: form, function, evolution*. Princeton, NJ: Princeton Univ. Press, 2000.

[11] Ellington C. P.: The aerodynamics of hovering insects flight. III Kinematics. *Philosophical Transactions of the Royal Society of London*. Series B. Biological Sciences, 305 (1122), 1984, pp. 41-78.

[12] Ellington C. P.: The novel aerodynamics of insect flight: applications to micro-air-vehicles, *The Journal of Experimental Biology*, 202, 1999, pp. 3439–3448.

[13] Fearing R., et all.: Wing transmission for a micromechanical flying insect, *Proc. IEEE Int. Conf. Robotics and Automation*, San Francisco, CA, Apr. 2000, pp. 1509–1516.

[14] Gessow A., Myers G. C.: *Aerodynamics of the helicopter*, College Park Press, 1985.

[15] Gnatzy W., Grünert U, and Bender M., Campaniform sensilla of *Calliphora vicina* (Insecta, Diptera). I. Topography, *Zoomorphology*, vol. 106, no. 5, 1987, pp. 312–319.

[16] Godbillon C.: *Dynamical systems on surfaces.* Berlin: Springer-Verlag, 1983.

[17] Goraj Z., Pietrucha J.: Basic mathematical relations of fluid dynamics for modified panel methods, *Journal. of Theoretical and Applied Mechanics*, vol. 36, no. 1, 1998, pp. 47-66.

[18] Gottlieb D. H.: Vector fields and classical theorems of topology, *Rendiconti del Seminario Matematico e Fisico di Milano*, vol. 60, 1990, pp. 193–203.

[19] Grünert U., Gnatzy W.: Campaniform sensilla of *Calliphora vicina* (Insecta, Diptera). II. Typology, *Zoomorphology*, vol. 106, no. 5, 1987, pp. 320–328.

[20] Hegstenberg R.: Multisensory control in insect oculomotor system, *Visual Motion and Its Role in the Stabilization of Gaze*, F. A. Miles and J. Wallman, Eds. Amsterdam: Elsevier, 1993, pp. 285–298.

[21] Kastberger R.: The ocelli control the flight course in honeybees, *Physiol. Entomol.*, vol. 15, 1990, pp. 337–346.

[22] Katz J., Plotkin A.: *Low-speed aerodynamics – from wing theory to panel methods*, McGrow-Hill, 2000.

[23] Keil T.A.: Functional morphology of insect mechnoreceptors, *Microscopy Res. Technique*, vol. 39, no. 6, 1997, pp. 506–531.

[24] Krapp H. G. Hegstenberg R.: Estimation of self-motion by optic flow processing in single visual interneurons, *Nature*, vol. 384, no. 6608, 1986, pp. 463–466.

[25] Lasek M, et all.: Analogies between rotary and flapping wings from control theory point of view, 2001, *AIAA paper no 2001-4002*.

[26] Lasek M, Sibilski K.; Analysis of flight dynamics and control of an Entomopter, *AIAA paper no 2003-5707,* 2003.

[27] Lasek M., et all.: A study of flight dynamics and automatic control of an animalopter, *Proc. of the 23rd International Congress of Aeronautical Sciences ICAS 2002, ICAS 2002-5.5.3 CP*, Toronto, 2002.

[28] Lasek M., Pietrucha J., Sibilski K.: Micro air vehicle manoeuvres as a control problem of flexible flapping wings, *AIAA Paper no. 2002-0526*, 2002.

[29] Lasek. M., Sibilski K., Modeling and simulation of flapping wing control for a micro-electromechanical flying insect (Entomopter), *AIAA 2002-4973 CP,* 2002.

[30] Marusak A., et all: Mathematical modelling of flying animals as aerial robots, *7th IEEE Inter. Conf. on Methods and Models in Automation and Robotics (MMAR 2001)*, Międzyzdroje, Poland, Aug. 28-31, 2001.

[31] Motazed B., D. Vos D., and M. Drela M.: Aerodynamics and flight control design for hovering MAVs, *Proc. American Control Conf.*, Evanston, IL, June 1998, pp. 681–683.

[32] Pornsin-Sisirak T., et all.: MEMS wing technology for a battery-powered ornithopter, *13th IEEE Inter. Conf. on Micro-Electro-Mechanical Systems (MEMS '00)*, Miyazaki, Japan, Jan. 23-27 2000.

[33] Sastry S.: *Nonlinear systems: analysis, stability, and control*. New York: Springer, 1999.

[34] Schenato L.: *Analysis and control of flapping flight: from biological to robotic insects*, PhD dissertation, University of California at Berkeley, 2003.

[35] Schenato L., Deng X., and Sastry S.: Hovering flight for a micromechanical flying insect: modeling and robust control synthesis, *15th IFAC World Congress Automatic Control*, Barcelona, Spain, July, 2002, pp. 235–240.

[36] Schenato L., Deng X., Wu W. C., Sastry S.: Virtual Insect Flight Simulator (VIFS): A software testbed of tnsect flight, *IEEE International Conference on Robotics and Automation*, Seoul, South Korea, May, 2001, pp. 3885–3892.

[37] Schenato L., Wu, W. and Sastry S.: Attitude control for a micromechanical flying insect via sensor output feedback, *IEEE Transactions on Robotics and Automation*, Vol. 20, No. 1, February, 2004.
[38] Schuppe H. and Hengstenberg R.: Optical properties of the ocelli of *Calliphora erythrocephala* and their role in the dorsal light response, *J. Compar. Biol. A*, vol. 173, 1993, pp. 143–149.
[39] Shyy W, Berg M and Ljungqvist D.: Flapping and flexible wings for biological and micro air vehicles, *Progress in Aerospace Sciences*, , Vol. 35, 1999, pp 455-505.
[40] Smith M. J. C., Wilkin P. J., Williams M. H.: The advantages of an unsteady panel method in modelling the aerodynamic forces on rigid flapping wings, *Journal of Experimental Biology*, 1996, Vol. 199, pp. 1073 - 1083.
[41] Strausfeld N. J.: *Atlas of an insect brain*. Berlin & New York, Springer-Verlag, 1976.
[42] Taylor C.: Contribution of compound eyes and ocelli to steering of locusts in flight: II. Timing changes in flight motor units, *J. Experimental Biol.*, vol. 93, 1981, pp. 19–31.
[43] Taylor C.: Contribution of compound eyes and ocelli to steering of locusts in flight: I. Behavioral analysis, *J. Experimental Biol.*, vol. 93, 1981, pp. 1–18.
[44] Taylor G. K. and Thomas A. L. R.: Dynamic flight stability in the desert locust *Schistocerca gregaria*, *J. Experimental Biology*, vol. 206, no. 16, 2003, pp. 2803–2829.
[45] Tobalske B. W., Dial K. P.: Flight kinematics of black-billed magpies and pigeons over a wide range of speeds, *Journal of Experimental Biol*ogy, 1996, Vol. 199, pp. 263 – 280.
[46] Willmott A. P., Ellington C. P.: The mechanics of flight in the hawkmoth manduca sexta. Part I. Kinematics of hovering and forward flight; *Journal of Experimental Biology*, no. 200, 1997, pp. 2705–2722.
[47] Wu W., et all.: Biomimetic sensor suite for flight control of a micromechanical flight insect: design and experimental results, *Proc. IEEE Int. Conf. Robotics and Automation*, vol. 1, Taipei, Taiwan, Sept. 2003, pp. 1146–1151.
[48] Yan J, et all.: Toward flapping wing control for a micromechanical flying insect, *Proc. IEEE Int. Conf. Robotics and Automation*, Seoul, South Korea, May, 2001, pp. 3901–3908.
[49] Żbikowski R.: Flapping wing technology, *Proc. European Military Rotorcraft Symp.*, Shrivenham, U.K., March 21–23, 2000, pp. 1–7.
[50] Żbikowski R.: On aerodynamic modeling of an insect-like flapping wing in hover for micro air vehicles, *Philosoph. Trans. Roy. Soc. London (Series A: Math., Physical and Eng. Scis.)*, vol. 360, no. 1791, 2002, pp. 273 – 290.

Copyright Statement